Kinetics of Butterfat Crystallization

D.S. Grall[a] and **R.W. Hartel**[b,*]

[a]Kraft General Foods, Glenview, Illinois 60025 and [b]Department of Food Science, University of Wisconsin, Madison, Wisconsin 53706

Fractionation of butterfat by melt crystallization is a commercial process in many countries for making butter fractions with varying melting, textural and flavor properties for use as food ingredients. However, the crystallization phenomena in this complex system are poorly understood and difficult to optimize and control. In this study, the crystallization kinetics of anhydrous butterfat were determined by cooling a melted sample to the final crystallization temperature in either a lab-scale (2 L) batch crystallizer or a pilot-scale (20 L) crystallization vessel. The butterfat was cooled sequentially from an initial temperature of 60°C to final temperatures of 30, 20 and 15°C at a constant cooling rate. Crystals formed at each temperature were separated by vacuum filtration, with the liquid cooled to the next crystallization temperature. Nucleation rates were determined by counting the number of crystals in a given volume of suspension during the course of crystallization. Crystal growth rates were obtained from image analysis of optical photomicrographs. Changes in viscosity, turbidity and mass of crystals also were determined. Effects of impeller velocity (75, 100 or 125 rpm) on the crystallization kinetics were determined. Nucleation and mass deposition rates increased while crystallization lag times decreased with increasing agitator velocities. Growth rates increased with agitator rpm at 20 and 15°C, but decreased with agitator rpm at 30°C, indicating different growth mechanisms. At 20 and 30°C, aggregation was the primary mechanism of crystal growth, whereas little aggregation was observed at 15°C. Crystallization at the larger scale, 20 L, showed only minor differences.

KEY WORDS: Butterfat, crystallization, fractionation, growth, kinetics, nucleation.

In the food industry, milkfat is a common ingredient in a variety of products including butter, ice cream and cheese. Milkfat (or butterfat), obtained from the process of fat removal from whole milk, possesses some unique compositional and functional characteristics. Milkfat contains a wide range of fatty acids, existing as triacylglycerols, including high amounts of both longer-chain fatty acids (C16 to C18) and shorter-chain acids (C4 to C10) (1). Over the past twenty years the consumption of milkfat has declined for several reasons, but mainly due to the negative health aspects surrounding its high concentration of saturated fats and cholesterol. Butterfat also possesses poor spreadability due to its high solid fat content at refrigerator temperatures (2).

Several methods for modifying milkfat have been investigated to increase its usage as a food ingredient. These include acyl exchange of the fatty acids on the triacylglycerol backbone, cholesterol reduction and fractionation. Fractionation, or separation of fat according to its physical properties, has been accomplished by various methods, including crystallization from the melt (3–5) or solvent (6,7), short-path distillation (8) and supercritical fluid extraction (9,10).

Many types of food products have been investigated for incorporation of milkfat fractions. If milkfat were to be fractionated on a commercial scale, it would be desirable that each of the fractions be utilized as a beneficial food ingredient. Some potential uses that have been investigated include cold spreadable butters and spreads (11–13), a cocoa butter replacement in chocolate (14,15), and as a food ingredient in puff pastries (16,17) and biscuits (15).

Crystallization from the melt is the process of phase transition of a molecule from a liquid to a solid state; in butterfat crystallization, the triacylglycerol molecules are arranged in a lattice structure. The driving force for crystallization from a pure melt is the difference between the melting point of the fat and the actual solution temperature. In mixed systems, the solubility of higher melting components in liquid oil also must be considered. Since the melting point of butterfat cannot be defined exactly due to its heterogeneous nature, the driving force for crystallization cannot be quantified. In addition, the relative solubilities of various triacylglycerides in the liquid oil have not been quantified.

Crystallization can generally be classified into two steps—nucleation and growth. Nucleation involves the initial formation of tiny embryonic crystals referred to as nuclei. Crystal growth involves diffusion of the flexible triacylglycerols from the bulk solution across a boundary layer, and incorporation into the crystal lattice structure of an existing crystal or nucleus (18). Because of the wide range of fatty acid constituents in milkfat, crystal growth is complicated by competition of similar, but incompatible, triacylglycerols, which either become incorporated into a mismatched lattice or diffuse back to the bulk solution. In either case, growth of existing crystals is slowed down due to the presence of multiple triacylglycerols. Crystallization of milkfat from the melt can be affected by various experimental conditions, including source and nature of the milkfat (19), agitation rate (20,21), scale of operation (22), final temperature (4) and rate of cooling (23). Higher yields of solid fraction were obtained by increasing the agitator velocity (24). Higher agitation velocities also gave small crystal size and a higher crystallization rate (21,25,26). A higher number of crystals appeared as the impeller velocity was increased, and the concentrations of large crystals (crystal diameter $> 250\ \mu m$) was smaller at higher rpm. The mechanisms for these effects have not been clearly defined.

Little work has been done in characterizing the effects of scale of operation on the crystallization process. Saxer and Fischer (22) summarized fractional crystallization of glycerides, including factors affecting the formation of fat crystals and a discussion of conditions required for all aspects of a commercial fractionation unit. For scaling up a pilot-scale system, the major considerations involve heat and mass transfer. The factors that affect the heat and mass transfer in the system include tank design, impeller design and method of cooling.

*To whom correspondence should be addressed.

The crystallization temperature affects the formation of the various polymorphs, the size of the crystals, composition of the solid fat and the physical properties of the fractions (3,4,25,26). Several researchers (3,25,27) have concluded that the temperature of crystallization has a small effect on the composition of triacylglycerols and their fatty acids. However, the physical properties of the fractions, including thermal melt properties and hardness values, were found to be significantly different at various crystallization temperatures. Thermal melt curves showed more distinct melting peaks in solid fractions crystallized above 28°C or below 6°C (11). Hardness values were considerably higher at higher crystallization temperatures for both fractions (25). Keogh and Higgins (24) crystallized milkfat at 25, 22 and 19°C and found that the crystallization temperature had the greatest effect on the slip point and yield of the fractions as compared with agitation time, cooling rate and initial temperature.

The effects of cooling rates were examined by deMan (23) and Schaap and Rutten (26), who found little difference in slip point, solid fat content, yield, hardness, thermal melting curves and fatty acid composition over the range from 0.01 to 1°C/min. However, Deffense (28) found that the cooling rate significantly altered the physical properties of the crystalline fractions at much higher cooling rates. As the cooling rate increased, the yield and drop point of the solid fraction decreased, while the crystal size increased. The basis for these effects was related to separation efficiency, although no specific mechanisms have been delineated.

Despite the numerous studies on melt crystallization of butterfat, there is little quantitative data on the kinetics of crystal formation and growth. The purpose of this study was to quantify the effects of various operating parameters on the crystallization kinetics of butterfat.

MATERIALS AND METHODS

Anhydrous milkfat was obtained from a local dairy in a 350-pound shipment. The milkfat, obtained in eight storage pails, was used for all experiments to provide consistency in fat composition. Samples were stored at 5°C until used.

For the 2-L experiments, approximately 2000 g of milkfat was placed in a 2.3-L stainless-steel jacketed vessel with a 30-cm height and a 10-cm inner diameter. The fat was held at 60°C by a circulating water bath for 0.5 h to ensure that all "crystal memory" had been lost. An impeller was attached to a Master Servodyne (Servodyne Controller, Chicago, IL) drive unit, which maintained constant motor speed so that viscosity changes of the solution, due to crystallization, resulted in motor torque changes. The impeller consisted of a 6-mm diameter stainless steel shaft with 4, 5-cm diameter, 45° pitched-blade impellers and 2 radial fins (dimensions of fins, 16 cm by 2 cm). The pitched-blade impellers were located at 1, 9, 17 and 25 cm from the bottom of the vessel and positioned to produce a lifting force when rotating. The crystallization vessel also was equipped with 4 baffles of 8.5 mm width, which extended through the full height of the tank. A copper-constantan thermocouple, attached to an aluminum brace and positioned 1 cm from the center of the tank and 14 cm from the bottom of the vessel, was used to determine solution temperature. Torque change and solution temperature were recorded with a data acquisition board attached to a microcomputer.

At the start of each experiment, the setpoint temperature of the Lauda water bath was reduced to the final crystallization temperature at constant agitator velocity of 125, 100 and 75 rpm. The average cooling rate of the water bath was 0.45°C/min for this system. Once the milkfat reached the crystallization temperature, 1-mL samples were removed at 15-min intervals and observed by photomicroscopy with a polarized-light microscope (Nikon Optiphot, Garden City, NY) equipped with a 35-mm camera. Sample collection was started when crystal nuclei were apparent under a magnification of 16 times (crystal diameter approximately 4 μm), all experiments were stopped after 22–24 h, and the slurries were filtered. Fractionation experiments were performed sequentially, *i.e.*, the liquid fraction obtained after separation was used for the next crystallization at the lower temperature. By this method four fractions were obtained, with three solid fractions at 30, 20 and 15°C and a liquid fraction at 15°C.

After the crystallization experiment was halted, the crystallization vessel was removed from the cooling bath (the water jacket was drained) and transferred to a temperature-controlled box that housed the filtration unit. The temperature of the box was maintained at the crystallization temperature by means of a circulating water bath in which water was circulated through a finned heat exchanger equipped with a blower to circulate air. Four 12.5-cm Buchner funnels were placed in a manifold made of 1.27-cm chlorinated poly-vinyl chloride (CPVC) pipe. The thickness of the filter cake was 1 cm for the 30 and 20°C fractions and 0.5 cm for the 15°C fractions. These thicknesses were used for consistency, and to ensure that the pressure drop across the cake did not reach levels that prevented good separation.

For the 20-L crystallization experiments, liquid milkfat was transferred to a 25-L crystallization tank (28 cm inner diameter by 41 cm height). The tank, made of stainless steel, was placed into a 30-gallon tank with a water temperature of 60°C and held for 0.5 h. The bath water was cooled at a constant rate of 0.25°C/min by using a cold-finger immersion cooler. The milkfat was agitated with a Master Servodyne drive unit similar to the Servodyne unit used for the small-scale crystallization experiments. However, torque readings were not recorded. The impeller unit consisted of a 9-mm stainless-steel shaft with an attached 20-cm 5-blade plastic impeller. The blade was placed 4 cm from the bottom of the tank with the blades rotating to lift the crystals. the agitation velocity was 75 rpm for all experiments. Solution temperature was monitored by placing a thermometer 4 cm below the surface of the milkfat.

Samples were taken for observation at 15-min intervals after the milkfat reached the crystallization temperature, with sample collection started when the first nuclei were observed microscopically at 16 times magnification. Experiments were ended after 24–26 h and the milkfat was filtered. Longer crystallization times were used, as compared to the bench-top scale, because of the slower cooling rate and the lower surface area per volume for heat transfer associated with the larger unit: $(\text{Surface area/volume})_{20\text{-L}} = 0.1738\ \text{cm}^{-1}$; $(\text{Surface area/volume})_{2\text{-L}} = 0.4948\ \text{cm}^{-1}$. At the end of each pilot-scale experiment, approximately 500 mL of the slurry was removed, weighed

and filtered to determine the final mass fraction of crystals (yield).

At the completion of the experiment, the crystallization vessel was removed from the water bath and placed in the temperature-controlled box (same as used in the small scale). The filtration device consisted of a modified sink (0.56 m by 0.53 m by .45 m height) with a rack placed 15.2 cm below the top. Four aluminum angle irons were used to support the rack, and a gasket with a width of 3.2 cm surrounded the edges. The filter cloth consisted of a woven polyester mesh with a retention rating of 25 μm. The effective surface area for filtration was approximately 2900 cm^2. The liquid oil was drawn into a sealed 10-gallon milk can evacuated by a vacuum pump. All fractions were stored in 5-gallon polystyrene containers at 5°C.

Sample measurements and analyses. Sample collection was started when the first crystal nuclei were observed. Samples were taken at 15-min intervals until the transmittance of light through a 5-mL sample at 490 nm reached zero. Sampling time intervals were then varied from 30–60 min up to about 600–800 min after the experiment was started. Several samples were taken at the end of the crystallization experiment between 1300–1500 min. All sampling equipment was kept near the crystallization temperature so that growth or melting of crystals would not be a factor as the sample was analyzed.

Nucleation rates were determined by counting the number of crystals falling in an engraved counting chamber. The counting chamber contained four cells with 10 calibrated engraved squares each (1 mm^2), with the area under the coverslip calibrated to 0.2 mm. A drop of slurry was placed in each cell and photomicrographs were taken at 8 times magnification. Eight pictures were required to cover the entire chamber, and crystals falling in the chamber engravings were visually counted from the photomicrographs and the number was multiplied by 125 to give a value for the number of crystals/mL. To prevent bias, crystals falling on the left and top engravings of each box were counted, while those falling on the right and bottom were not. Nucleation rates were obtained by determining the slope of the initial portion of the crystal number curve.

Photomicrographs of growing fat crystals, under polarized light, were taken during the course of each experiment. Polarized light was useful for crystal definition and for observation of uniformity of crystals. Samples of approximately 1 mL were placed on a slide with a coverslip and pictures were taken at magnifications of 8 or 16 times. The crystals formed at 30 and 15°C were relatively small so that 16 times magnification was required, whereas the crystals that formed at 20°C were much larger and were photographed at a magnification of 8 times to obtain a large sample size. Four to eight photographs were taken for each sample to ensure a sufficient sample size. The perimeter of each crystal in the photomicrographs was manually traced by means of a digitizer board, with the results being automatically transferred to a microcomputer. Crystal area (μm^2) was collected by image analysis software, and equivalent circular diameters (diameter of a circle having an equivalent area to the measured area) and crystal size distributions (mean size and variance) were calculated with a custom-made program written in Basic. The number of crystals counted was between 200–350 crystals per sample. The value of 200 was selected for the crystals produced at 30°C because the low number of crystals per photomicrograph made it difficult to obtain a higher sample number and remain within eight photomicrographs for each sample time. The population-based mean diameter, L, for each distribution was plotted *vs.* crystallization time, and the growth rate was obtained from the linear portion of the curve.

Two methods were used to determine the suspension density (or crystal mass)—microfiltration and turbidity. For microfiltration, 1.5 mL of solution was drawn into a 3-mL syringe and injected into a 25-mm filter holder through a filter membrane. After injection, the syringe was removed and a vacuum tube was attached for 3 min. The filtering apparatus was weighed before and after loading the sample and after the sample had been injected. Because of the small volume used, the liquid oil could not be collected efficiently for weighing, and the mass balance could not be closed. To account for liquid oil remaining in the filtering apparatus, three liquid oil samples, taken before crystallization started, were injected through the filtering apparatus, and the mass of entrained oil was calculated. The assumption was made that the amount of oil entrained by the apparatus would not change significantly, so that this average value was subtracted from each sample to determine mass fractions. Solid fractions found in this way (microfiltration) at the end of the experiment compared favorably with mass fraction calculations made upon filtering the entire solution.

Changes in suspension density were measured by transmittance of light at 490 nm through a 5-mL sample. This wavelength was chosen because of the peak in transmittance observed for whole milkfat. A clear liquid standard was prepared for each experiment from the milkfat being crystallized. Correlations for light scattering, where the extinction of light is a combination of scattering and absorption, are given as (29):

$$I/I_o = e^{-\gamma_e l} \quad [1]$$

where I_o is the intensity incident upon the first surface; I, intensity transmitted through a path thickness, l; I/I_o, transmittance of light through the sample; and γ_e, extinction coefficient. The extinction coefficient can be defined by:

$$\gamma_e = c\ B_{ext} \quad [2]$$

where c is the number of particles per unit volume of solution; and B_{ext}, area of light blocked by one average-sized particle.

Beer's law for absorbance can be modified to include light scattering by substituting Eqs. [1] and [2] into an overall absorbance equation:

$$A = \log (I_o/I) = \log (e^{c\ B_{ext} \cdot l}) \quad [3]$$

where A is the overall extinction of light through the sample, including scattering effects and particle absorbance. Rearrangement of the right-hand side of Eq. [3] gives:

$$A = \frac{c\ B_{ext} \cdot l}{2.303} \quad [4]$$

For a crystallization process, the value for B_{ext} will change as the crystal diameter changes, and thus the

amount of light that is absorbed or scattered is proportional to the concentration of particles in solution and the average area of the particle distribution. Rate equations for crystallization could be derived from the absorbance values and given by:

$$\frac{dA}{dt} = B_{ext}\, k_c \frac{dc}{dt} + c\, k_c \frac{dB_{ext}}{dt} \quad [5]$$

where k_c is a constant. During the initial nucleation phase the change in crystal area over time (related to B_{ext}) may be considered negligible compared to the change in concentration of particles, and Eq. [5] can be written as:

$$\frac{dA}{dt} = k_c' \frac{dc}{dt} \quad [6]$$

where $k_c' = k_c\, B_{ext}$. Eq. [6] shows that the extinction of light due to light scattering and absorbance is proportional to the concentration of particles in solution. The slopes were determined for the initial linear portion of both the mass fraction and absorbance curves. In all cases, the slopes of absorbance with time curves were found to be identical to curves of microfiltration data *vs.* time. The combined average of mass deposition rates found from microfiltration data and absorbance were used.

Fatty acid analysis. The composition of fatty acids in the milkfat fractions was determined by gas chromatography. Butyl esters were produced by a modified method of Iverson and Sheppard (30). Samples were injected into the gas chromatograph and the concentration of each ester was determined by peak area analysis.

Thermal heating curves. Thermal heating curves were determined for each fraction, in duplicate, in a Perkin Elmer DSC 7 differential scanning calorimeter (Perkin Elmer, Norwalk, CT) with liquid nitrogen as a heat sink. The samples were initially cooled to −40°C. A constant temperature ramp of 10°C/min was used for all samples over the temperature range between −40–80°C.

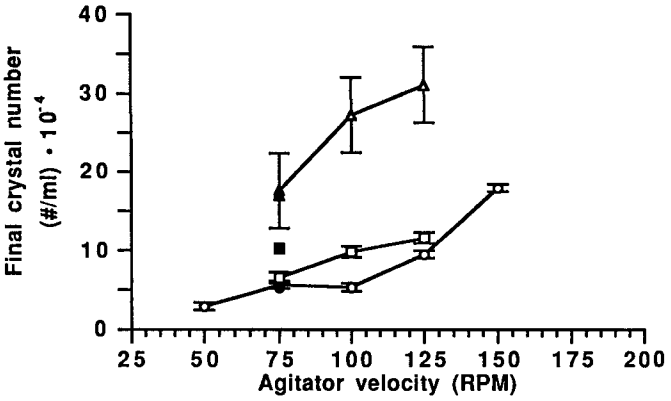

FIG. 1. Comparison of final crystal number with agitator velocity for batch crystallization of butterfat. Open circle, 2-L, 30°C, 0.45°C/min; □, 2-L, 20°C, 0.45°C/min; △, 2-L, 15°C, 0.45°/min; ●, 20-L, 30°C, 0.25°C/min; ■, 20-L, 20°C, 0.25°C/min; and ▲, 20-L, 15°C, 0.25°C/min.

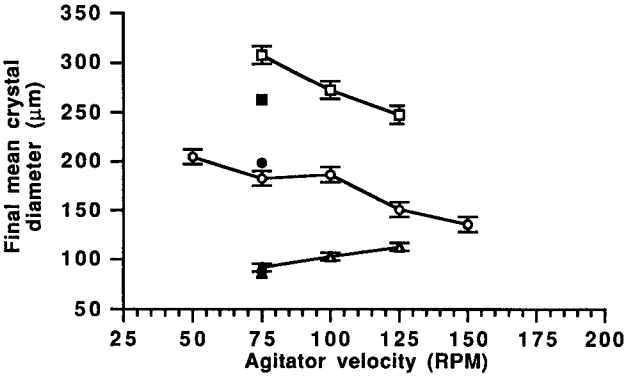

FIG. 2. Comparison of final mean crystal diameter with agitator velocity for batch crystallization of butterfat. Symbols as in Figure 1.

RESULTS AND DISCUSSION

Morphology. Photomicrographs taken of the growing crystals demonstrate the extreme differences in crystal structure. The crystals formed at 30°C consisted of a conglomeration of needle-like structures. The crystals at 20°C did not show these needle-like structures at the magnifications used, but appeared to be a conglomeration of smaller, tighter aggregates. During the crystallization process, partially joined crystals were observed for both the 30 and 20°C fractions. The crystals at 15°C formed uniform spheres with a single birefringent cross in polarized light, which indicated a more uniform structure.

Crystal number and mean size. The final crystal number and final mean diameter, which would affect the yield of solids, were plotted for each experimental condition (see Figs. 1 and 2). Figure 1 shows that the final crystal number increased with agitator velocity with the greatest effect at 15°C. The final mean crystal diameter (Fig. 2) was found to decrease with agitator velocity at 30 and 20°C, but increased at 15°C. This would indicate that the crystals at 15°C were not easily sheared by the higher impeller rpm.

Fraction yields. The yield of solid fat varied with agitator velocity and crystallization temperature, as shown in Figure 3. This mass of solid fat also includes the mass of liquid oil remaining in the crystals, which has been noted as a major problem associated with melt crystallization. The amount of entrained oil varies with experimental conditions, including crystallization temperature, agitator velocity and cooling rate, although this is difficult to determine directly. The mass of crystals increased with increasing rpm, with the largest effect seen for the solid fraction at 15°C and the smallest effect at 20°C. These differences may be partly caused by the effects of rpm on crystallization conditions that affect the level of liquid entrainment during filtration. These effects include number, mean size and shape of crystals.

Kinetics of crystallization. The kinetics of crystallization were determined by various experimental methods. Nucleation, mass deposition and growth rates were determined by calculating the slope of the initial linear portion of the respective curves. Lag times for nucleation and mass deposition were determined by calculation from a slope-intercept equation. The nucleation values gave the rate at which particles formed in the solution during the initial nucleation phase, and the growth data determined the increase in mean crystal diameter over the initial

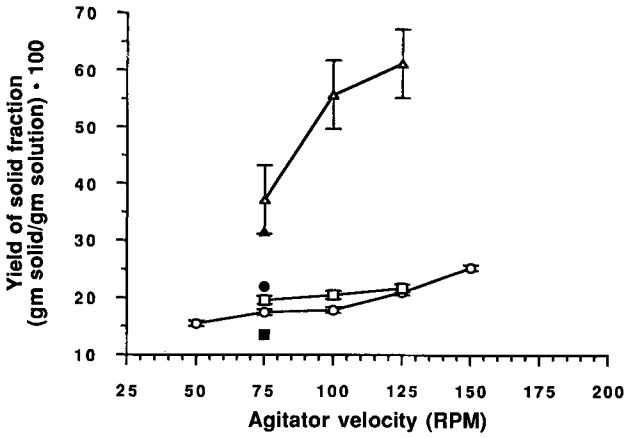

FIG. 3. Yield of solid fraction at various agitator velocities for batch crystallization of butterfat. Symbols as in Figure 1.

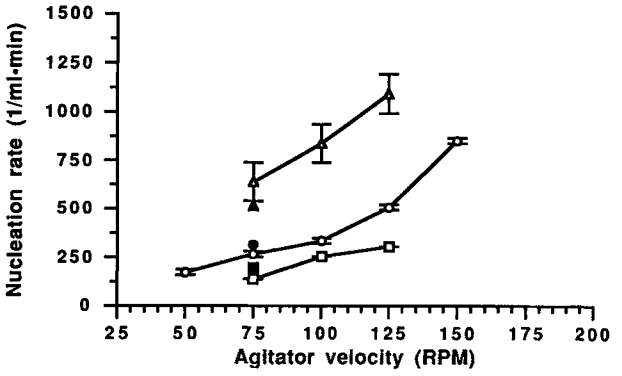

FIG. 5. Comparison of nucleation rates at various agitator velocities for batch crystallization of butterfat. Symbols as in Figure 1.

growth phase. The mass deposition data gave the rate of formation of total solids, which combines both nucleation and growth rates. Replicates of each experiment were made to ensure reproducibility at each condition, and the standard error was calculated for each method by pooling the standard error of the individual experiments at each crystallization temperature (31).

Nucleation. A typical temperature-time profile along with the nucleation curve is shown in Figure 4 for a crystallization temperature of 20°C. Similar curves were observed at the other conditions. The number of nuclei per milliliter showed a linear increase after an initial lag time for all conditions. For all crystallization temperatures, the solution temperature increased at the onset of nucleation, decreased slightly and, after a period of time, dropped off to the water bath temperature. The two phases may indicate the initial rapid rates of nucleation and growth, followed by slower rates as the system approached equilibrium.

The influence of agitator velocities on the nucleation rate, as measured by the initial slope of particle number with time, can be seen in Figure 5, and the lag time associated with nucleation in Figure 6. In the 2-L crystallizer, the nucleation rates were highest for crystals formed at 15°C, for the agitator velocities tested, and lowest for crystallization at 20°C, while the lag times were longest at 15°C and shortest at 30°C. The increase in nucleation rate with agitation velocity for all temperatures could be explained by the increase in impeller shear associated with higher agitator velocity. This higher shear promotes secondary nucleation, where the impeller blades caused tiny crystals to form from disruption of existing crystals. The decrease in lag time with increased rpm's also can be explained by increased impeller shear, which would promote crystallization at a faster rate at the same sub-cooled temperature.

For the 20-L crystallizer, the trend for nucleation rate was consistent with that of the 2-L experiments. This suggests that the variations in equipment, which would effect the heat and mass transfer conditions, had no significant effect on the rate of nucleation. The lag times were slightly shorter for crystallization temperatures of 15 and 30°C, but remained nearly the same for 20°C. The shorter lag times could be caused by the five-blade impeller used for the pilot-scale experiment, which produced a higher local shear rate and may have enhanced heat transfer.

Crystal growth. Growth rates were determined from the linear portion of the growth curve where the mean equivalent circular diameter was plotted over time. Growth rates for crystals formed at 15 and 20°C increased with increasing agitator velocities, while the growth rate for

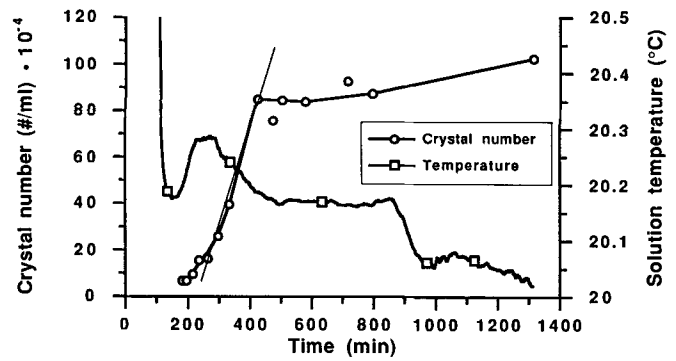

FIG. 4. Number of crystals and solution-temperature during batch crystallization of butterfat (2-L, 100 rpm, 20°C, 0.45°C/min cooling rate).

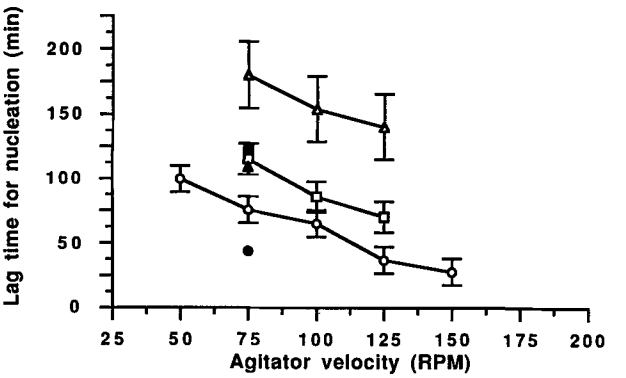

FIG. 6. Comparison of lag times associated with nucleation for batch crystallization of butterfat. Symbols as in Figure 1.

the 30°C crystallization initially increased between 50 and 100 rpm, and then decreased with increasing agitator velocity (Fig. 7). This trend suggests that the crystals formed at 30°C were held together in loose aggregates. At 30°C, the initial crystals formed as needles, which subsequently aggregated into loosely-packed structures. Thus, the mechanism for growth in this fraction was mainly by aggregation of existing crystals. Lower agitation velocities promote a shear aggregation, while higher agitator velocities slow this aggregation process by preventing the crystals from aligning themselves for attachment with adjacent crystals. In addition, higher shear rates tend to disrupt aggregates that do form. The crystals formed at 15 and 20°C appear to grow by another mechanism because growth rates for these fractions increased with increasing agitator velocities. This growth would be on a molecular level where individual triacylglycerols are incorporated into the crystal lattice from the bulk solution. Photomicroscopy showed that the 20°C crystals were compacted clumps of smaller crystals with a higher affinity for one another. One would expect that the crystal growth rate would eventually reach a maximum and then decrease for these fractions with increasing agitator rpm because some aggregation was evident. However, sufficiently high agitator speeds were not obtained. In addition, heat and mass transfer effects may be more important for these crystals, where increased agitator speed may result in increased growth rates. Similar results, but to a lesser degree, were observed for crystals grown at 15°C. Uniform spherical crystals formed with no aggregation present.

From the pilot-scale experiments, the growth rates followed similar trends at 30 and 15°C, compared to the small-scale results, while crystallization at 20°C gave a significantly higher growth rate. Perhaps this was due to larger effects of heat and mass transfer at this condition, although it is unclear exactly how this might occur. This anomalously high growth rate at 20°C in the 20-L crystallizer is difficult to explain.

Mass deposition rate. Mass deposition rates were calculated from turbidity measurements and microfiltration data. Mass deposition rate, which is influenced by both nucleation and growth rates, gives a value for the total amount of solid fat formed over time. The mass deposition was determined from turbidity measurements by determining the absorbance of light through the crystalline butterfat and adjusting the value by multiplying the actual mass fraction of crystals determined by microfiltration. The mass deposition rates were similar for microfiltration and turbidity, so the values were pooled to obtain a single mass deposition rate at each experimental condition.

The effects of agitator velocity on mass deposition rate can be seen in Figure 8. Mass deposition rates increased with agitator velocity for all temperatures, with the greatest effect at 15°C and the least at 20°C. These trends also were consistent with final solid yield (see Fig. 3). Mass deposition rate should follow the combined trends of nucleation and growth with agitator velocity, although crystal size and number also are important. At a crystallization temperature of 15°C, the nucleation rate increased the most, with the smallest increase in the growth rate. The mass deposition increase can then be accounted for by the large increase in the number of particles. For the 20°C fraction, the nucleation rate showed a small increase, and the growth rate increased dramatically with increasing agitator velocity. Thus, an increase in mass deposition rate with agitation velocity was observed.

Thermal curves. The thermal curves, as determined by differential scanning calorimetry, are given in Figure 9.

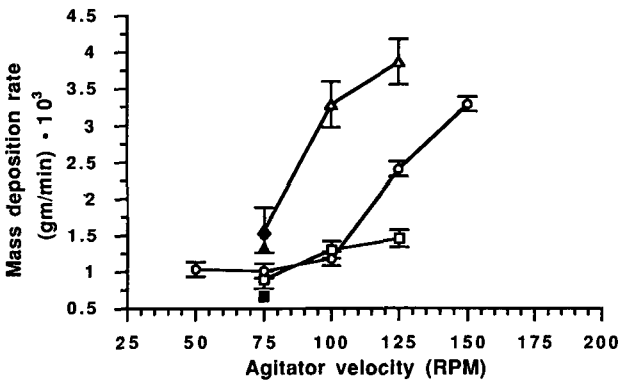

FIG. 8. Comparison of mass deposition rates at various agitation velocities for batch crystallization of butterfat. Symbols as in Figure 1.

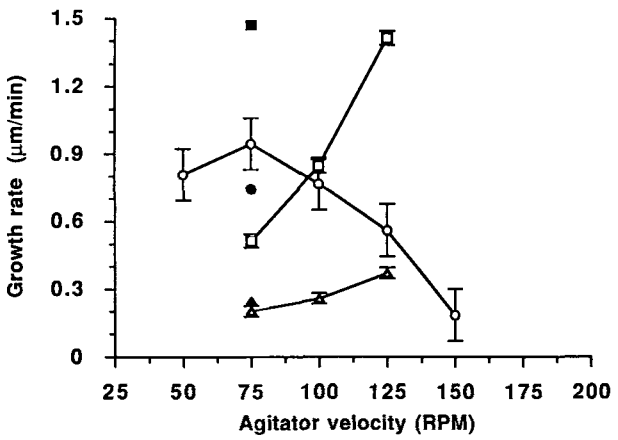

FIG. 7. Comparison of growth rates at various agitator velocities during batch crystallization of butterfat. Symbols as in Figure 1.

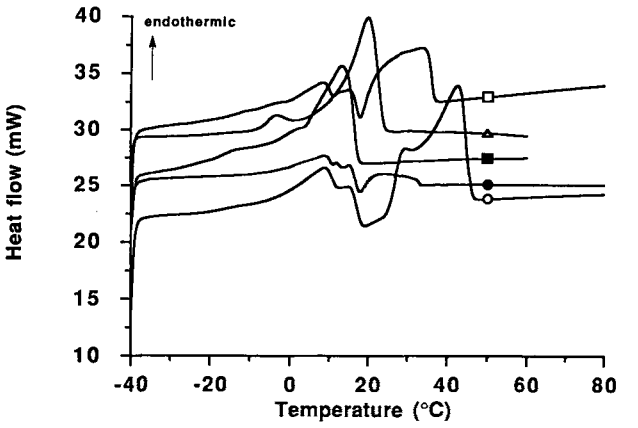

FIG. 9. Comparison of thermal curves for butterfat and its fractions crystallized from the melt. ●, Whole milkfat; ○, solid at 30°C; □, solid at 20°C; △, solid at 15°C; and ■, liquid at 15°C.

TABLE 1

Melting Points of Milkfat and Its Fractions

Sample	m.p. (°C)
Whole milkfat	33.1
Solid at 30°C (HMF)	43.0
Solid at 20°C (MMF)	33.9
Solid at 15°C (LMF)	19.5
Liquid at 15°C (VLMF)	12.5

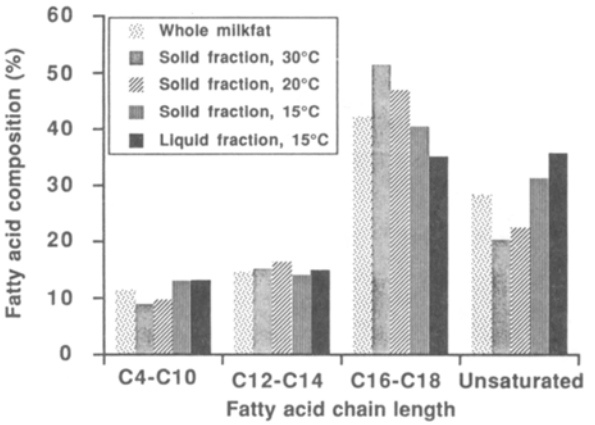

FIG. 10. Fatty acid profiles for butterfat and its fractions crystallized from the melt.

An estimation of the melting points of the fractions, based on peak temperatures, are given in Table 1. The thermal heating curve for whole milkfat shows a wide range of melting, while each fraction gave a more distinct peak in the heat flow. The medium melting fat (MMF) gave a similar melting curve to the whole milkfat. The high (H)MF melting curve showed two peaks at 41 and 8°C, while the low (L)MF and very low (VL)MF fractions gradually melted starting at −20°C with a peak at the melting point of the sample.

Fatty acid analysis. The fatty acid analysis of the milkfat fractions can be seen in Figure 10. The fatty acids obtained from the milkfat triacylglycerols were grouped into four categories: Short-chain acids (C4:0–C10:0), medium-chain acids (C12:0–C14:0), long-chain acids (C16:0–C18:0) and the *cis*-unsaturated fatty acids (C14:1–C18:2). Similar to results from the literature (19,28), no major compositional differences were evident. There was a general trend with the shorter-chain and unsaturated fatty acids migrating to the lower melting fractions, and the longer-chain fatty acids to the higher melting fractions. Despite the small differences in the fatty acid content of the fractions, the melting point differences were significant. This is most likely due to the positional locations of fatty acids in the triacylglycerols, which affects the physical properties, including crystallization and melting.

ACKNOWLEDGMENTS

This work was supported by the Wisconsin Milk Marketing Board through the Wisconsin Center for Dairy Research.

REFERENCES

1. Lindsay, R.C., *Fractionation and Functionality Characterization of Milkfat to Expand its Use in Contemporary Food Applications*, American Dairy Science Association, North Carolina State University, Raleigh, 1990.
2. Fouad, F.M., F.R. van de Voort, W.D. Marshall and P.G. Farrell, *J. Am. Oil Chem. Soc. 67*:981 (1990).
3. Amer, M.A., D.B. Kupranycz and B.E. Baker, *Ibid. 62*:1551 (1985).
4. Antila, V., *Milk Industry 81*:17 (1979).
5. Badings, H.T., J.E. Schaap, C. DeJong and H.G. Hagerdoorn, *Milchwissenschaft 38*:95 (1983).
6. Sherbon, J.W., and R.M. Dolby, *J. of Dairy Sci. 56*:52 (1973).
7. Schaap, J.E., H.T. Badings, D.G. Schmidt and E. Frede, *Netherland Milk Dairy Journal 29*:242 (1975).
8. Arul, J., A. Boudreau, J. Makhlouf, R. Tardif and T. Bellavia, *J. Am. Oil Chem. Soc. 65*:1642 (1988).
9. Kankare, V., V. Antila, T. Harvala and V. Komppa, *Milchwissenschaft 44*:407 (1989).
10. Arul, J., A. Boudreau, J. Maklouf, R. Tardif and M.R. Sahasrabudhe, *J. Food Sci. 52*:1231 (1987).
11. Jamotte, P., and A. Guyot, *Preparation and Use of New Types of Butter Fats Modified by Fractional Crystallization in the Absence of Solvents*, Dairy Station, Gembloux, No. B.01, 1980.
12. Kankare, V., and V. Antila, *Fat Sci. Tech. 5*:171 (1988).
13. Verhagen, L.A.M., and J. Bodor, U.S. Patent no. 4,438,149 (1984).
14. Timms, R.E., and J.V. Parekh, *Lebensm.-Wiss. u.-Technol. 13*:177 (1980).
15. Jordan, M.A., *Studies on Butter Oil*, British Food Manufacturing Industries Research Association, Leatherhead, England, No. 568, October, 1986.
16. Seibel, W., *Zucker-und-Süsswarenwirtschaft 40*:124 (1987).
17. Schaap, J.E., and J.C. Kim, *Zuivelzicht 73*:137 (1981).
18. Walstra, P., in *Food Structure and Behaviour*, edited by J. Banshard, Academic Press Limited, London, 1987.
19. Badings, H.T., J.E. Schaap, C. DeJong and H.G. Hagerdoorn, *Milchwissenschaft 38*:150 (1983).
20. Cole, B.J., M.S. Thesis, Massey University, 1990.
21. Black, R.G., *Aust. J. Dairy Tech. 30*:153 (1975).
22. Saxer, K., and O. Fischer, in *Progress in Food Engineering*, edited by C. Cantarelli, Forster-Verlag Ltd., Switzerland, 1983.
23. deMan, J.M., *Can. Inst. Food Techn. J. 1*:90 (1968).
24. Keogh, M.K., and A.C. Higgins, *Irish Journal of Food Science and Technology 10*:35 (1986).
25. Foley, J., and J.P. Brady, *J. Dairy Res. 51*:579 (1984).
26. Schaap, J.E., and G.A.M. Rutten, *Netherlands Milk Dairy Journal 30*:197 (1976).
27. Tirtiaux, A., *J. Am. Oil Chem. Soc. 60*:425A (1983).
28. Deffense, E., *Fat Sci. Techn. 13* (1987).
29. van de Hulst, H.C., *Light Scattering by Small Particles* (Third edn.), John Wiley and Sons, Inc., London, 1957.
30. Iverson, J.L., and A.J. Sheppard, *Food Chemistry, 21*:223 (1986).
31. Ott, L., *An Introduction to Statistical Methods and Data Analysis* (Third edn.), PWS-KENT Publishing Co., Boston, 1988.

[Received December 16, 1991; accepted March 30, 1992]